

UCSF

UC San Francisco Previously Published Works

Title

Craniofacial diversification in the domestic pigeon and the evolution of the avian skull.

Permalink

<https://escholarship.org/uc/item/0nb6s619>

Journal

Nature ecology & evolution, 1(4)

ISSN

2397-334X

Authors

Young, Nathan M
Linde-Medina, Marta
Fondon, John W
et al.

Publication Date

2017-03-01

DOI

10.1038/s41559-017-0095

Peer reviewed



Published in final edited form as:

Nat Ecol Evol. ; 1(4): 95. doi:10.1038/s41559-017-0095.

Craniofacial diversification in the domestic pigeon and the evolution of the avian skull

Nathan M. Young^{1,*}, Marta Linde-Medina¹, John W. Fondon III², Benedikt Hallgrímsson³, and Ralph S. Marcucio¹

¹University of California San Francisco, Department of Orthopaedic Surgery, 2550 23rd Street, San Francisco, California 94115

²University of Texas at Arlington, Department of Biological Sciences

³University of Calgary, Department of Cell Biology and Anatomy and the Alberta Children's Hospital Research Institute

Abstract

A central question in evolutionary developmental biology is how highly conserved developmental systems can generate the remarkable phenotypic diversity observed among distantly related species. In part, this paradox reflects our limited knowledge about the potential for species to both respond to selection and generate novel variation. Consequently, the developmental links between small-scale microevolutionary variations within populations to larger macroevolutionary patterns among species remains unbridged. Domesticated species such as the pigeon are unique resources for addressing this question because a history of strong artificial selection has significantly increased morphological diversity, offering a direct comparison of the developmental potential of a single species to broader evolutionary patterns. Here we demonstrate that patterns of variation and covariation within and between the face and braincase in domesticated breeds of the pigeon are predictive of avian cranial evolution. These results indicate that selection on variation generated by a conserved developmental system is sufficient to explain the evolution of crania as different in shape as the albatross or eagle, parakeet or hummingbird. These “rules” of craniofacial variation are a common pattern in the evolution of a broad diversity of vertebrate species, and may ultimately reflect structural limitations of a shared embryonic bauplan on functional variation.

“We may look in vain through the 288 known species [of pigeons and doves] for a beak so small and conical as that of the short-faced tumbler; for one so broad and short as that of the barb; for one so long, straight, and narrow...as that of the English carrier...”¹

Users may view, print, copy, and download text and data-mine the content in such documents, for the purposes of academic research, subject always to the full Conditions of use:http://www.nature.com/authors/editorial_policies/license.html#terms

*Senior and Corresponding Author: nathan.young@ucsf.edu.

Author contributions: NY designed the research. NY and JF collected pigeon specimens. NY and ML performed the analyses. NY, ML, BH, and RM contributed to the interpretation of the results. NY drafted the paper. All authors contributed to the final version.

Supplementary information is provided.

Competing interests: The authors declare no competing financial interests.

Domesticated animals have long played an important role in our understanding of the evolution and diversification of natural species. One of Darwin's² key insights was that domesticates provided an analogous and accelerated window into the vastly slower process of natural selection, accomplishing in generations what may normally take millions of years. One species in particular, the common pigeon, was central to his understanding of selection and its role in evolution. Among other traits^{3,4}, Darwin noted how the shape of the pigeon's head and beak has been subjected to extensive selection by humans⁵, resulting in breeds that qualitatively exceed variation seen not only within a single wild bird species, but also converge on phylogenetically distant avians (FIG. 1 and Supplementary Fig. 1).

Darwin believed selection was the primary force driving breed and species diversification, but he also observed how the “correlation of growth among body parts” could confound the breeder's goals^{1,5}. That said, he was largely unaware of how these rules were determined or how they might ultimately impact phenotypic diversification. In the modern view, genetic pleiotropy drives covariation^{6,7} through the correlated effects of variation in developmental processes⁸, in turn biasing the long-term direction and magnitude of evolutionary responses to selection^{9,10}. That said, there is continued debate about the relative importance of development and selection to the patterning of macroevolutionary diversity since evolutionary changes can occur in both the distribution of variation across such processes and in the developmental basis for the correlations themselves⁸. Consequently, selection not only impacts observed phenotypic distributions, but can also alter the rules for how variation is generated within the “space” in which phenotypes exist^{11,12}.

In this context, the dramatic variation among domesticated pigeon breeds provides critical evidence not only of selection, but also a unique window into how the developmental potential of a single species corresponds to evolutionary diversification. Avian diversity is driven by myriad functional factors that are particular to lineages and contingent within the history of each group. If the diversity of morphology generated within a single bird species were to resemble that produced by evolution among all birds, then this would provide powerful evidence for the existence of key developmental drivers of correlations among parts that persist across broad ranges of phylogenetic diversity. Despite the potential importance of domestic breeds to these questions, there have been few attempts to either characterize skeletal variation in the pigeon¹³, or relate them to broader avian radiations¹⁴. Here, we test whether differences in morphological variation among avians and domestic and feral pigeon populations reflect changes in the organization of cranial covariation, as measured in terms of pattern and magnitude of integration and modularity, or if instead variation within and among these groups reflects the potential of a common developmental system to generate phenotypic diversity.

Results

We first compared feral and domestic pigeons to proxies of the wildtype ancestral populations, the rock dove. Linear data for rock doves and feral and domestic pigeons (Supplementary Tab. 1) was significantly correlated with overall body size. All groups overlapped, and there were no significant differences in slope, with the exception of premaxilla and cranial width in domestics (Supplementary Fig. 2). In all dimensions

domestics exhibit increased mean and variance (Levene's test, $p < 0.0001$), with the average coefficient of variation across traits three times greater than estimated for feral populations ($CV_{\text{dom}} = 13.3\%$, $CV_{\text{fer}} = 4.5\%$), and nearly four times that of the wild rock dove ($CV_{\text{rd}} = 3.6\%$) (Supplementary Tab. 2). Ferals are more variable in some traits (premaxilla and skull width, overall size) relative to the rock dove (Levene's test, $p < 0.05$), but not others (premaxilla and mandible length) (Levene's test, $p > 0.05$), in part due to geographic population heterogeneity. Increased variation in domestics was generally consistent with predictions of the rock dove within-group regression, with the exception of width. The first axis of the Principal Components Analysis (PC1, 81.5% variation) was significantly associated with size (geometric mean) ($r^2 = 0.958$, $p < 0.0001$), with no significant difference in slope among groups ($p = 0.522$) (FIG. 2). The pattern of trait correlations among pigeons is highly significant when adjusted for repeatability ($r_m > 1$ between rock dove and domestic ($p < 0.0001$); $r_m = 0.798$ for the feral-domestic comparison ($p < 0.0001$)) (Supplementary Tab. 3). The unadjusted VE of the domestics is significantly higher than wild doves and pigeons, but is statistically indistinguishable from the rock dove at comparable CV values (e.g., when $CV = 3$, $VE_{\text{dove}} = 0.56$ and $VE_{\text{dom}} = 0.62$), and converges with all wildtypes when $CV = 6$. Together these results suggest that domestics have increased magnitude of variation produced by a trait correlation structure shared with wild pigeons.

Next, we turned to the pigeon shape data. Here, brain~shape allometry accounted for 20.2% of total variation ($p < 0.001$), with smaller individuals having proportionately shorter, straighter beaks and wider crania (Supplementary Fig. 3). The first three PCs of non-allometric pigeon cranial shape variation describe facial length (PC1, 64.2% variation), beak and cranial flexion (PC2, 16.7% variation), and facial width (PC3, 5.4% variation), altogether accounting for 86.4% of total shape variation (FIG. 3). The matrix correlation between feral and domestic shape data was significant ($r_m = 0.549$, $p < 0.0001$), suggesting a similar covariance structure. This result was further confirmed by a significant non-random alignment between PC1-4 eigenvectors ($p < 0.001$) (Supplementary Tab. 4). Feral and domestic pigeons overlap in shapespace, although Procrustes configurations of domestics account for a larger proportion of landmark variance compared to ferals (Levene's test, $p < 0.001$) (Supplementary Fig. 4). Domestic pigeon faces exhibit $\sim 8\times$ higher landmark variance compared to ferals, while braincase configurations are $\sim 4\times$ more variable. Partial Least Squares (PLS) analysis between face and braincase shape indicates that almost all their covariation can be explained in the first axis (94.4%, $p < 0.001$) (Supplementary Tab. 5), which describes a narrowing of the braincase with increasing facial length (FIG. 4).

Finally, we compared pigeon shape data to the avian radiation. Here, brain~shape allometry accounted for 10.0% of avian shape variation and was weakly non-significant ($p = 0.091$) (Supplementary Fig. 3). Allometric variation was associated with curvature of the beak and skull base but not with beak length, in contrast to pigeons. PCA of the non-allometric avian data decomposed cranial shape into premaxilla length (PC1, 44.4%), skull flexion (PC2, 27.4%), and facial width (PC3: 7.5%) (FIG. 5 and Supplementary Fig. 5). There is evidence of significant phylogenetic signal within this shapespace ($K = 0.895$, $p = 0.042$) (Supplementary Fig. 6), with feral pigeons most closely aligned with the fruit dove, and domestic breeds distributed in a space overlapping ferals, the fruit dove, and the shorter beaked parakeet. The avian shapespace exhibits a strong correspondence to the pigeon shape

covariance structure as a whole ($r_m=0.851$, $p<0.001$), and individually to ferals ($r_m=0.510$, $p<0.001$) and domestics ($r_m=0.777$, $p<0.001$). Pigeon and avian shapespaces exhibit non-random alignment (PC1: 25.2° , $r_v=0.91$, $p<0.0001$; PC2: 55.9° , $r_v=0.56$, $p<0.0001$; PC3: 56.7° , $r_v=0.55$, $p<0.0001$) (Supplementary Tab. 4). Avians exhibit higher disparity ($\sim 1.5\times$) and landmark variance ($\sim 3\times$) compared to domestic pigeons (Supplementary Fig. 4). RV and CR coefficients for hypothesized face-braincase modules in avians (RV=0.76, $p=0.098$; CR=0.939, $p=0.005$; r-PLS=0.924, $p=0.001$), ferals (RV=0.46, $p<0.001$; CR=0.868, $p=0.010$; r-PLS=0.845, $p=0.030$), and domestic pigeons (RV=0.91, $p=0.006$; CR=1.029, $p=0.010$; r-PLS=0.978, $p=0.001$) were all significant, suggesting strong shape integration (FIG. 4 and Supplementary Fig. 7). However, both measures were generally less than or equal to random module partitions of the dataset, suggesting greater covariation within hypothesized modules than between, consistent with modularity. PLS analysis of all avian data (RV=0.820, $p<0.001$) further confirms that 88.8% of the covariation between face and braincase shape is associated with neurocranial width and facial length (PLS1, $r=0.938$, $p<0.001$) (Supplementary Tab. 5), and is similar to the pattern of integration found within pigeons (PLS1, 23.4° , $r_v=0.918$, $p<0.0001$).

Discussion

These results demonstrate that under a regime of strong artificial selection, domestic pigeons recapitulate the principal axes of avian craniofacial shape variation, but not the magnitude. Importantly, domestic pigeons have increased the relative contributions of the same determinants of covariation that influence evolutionary diversification among avians, even though there is no reason to predict *a priori* that the direction of selection on functional demands in different species of birds should be similar to those of human breeders. This result indicates that both pigeon breeds and avians have diversified utilizing a common pattern of integration and modularity between the face and braincase, resulting in allometric and integrated non-allometric variation associated with length, curvature, and width. While face and braincase shape are strongly integrated, changes in facial shape are accompanied by predictable but relatively small corresponding changes in braincase shape, which accounts for the greater diversity of beak shapes compared to brains. Together these results imply that avian craniofacial diversity is a product of selection on primitive patterns of variation and covariation between the face and braincase that are defined by a developmental system common to all birds, and which has undergone little change during avian evolutionary diversification.

This analysis samples a broad diversity of living birds, with species distributed across shapespace. That said, examination of predicted shapes from relatively unoccupied regions suggests that some potential outcomes may be less likely due to a mixture of developmental and functional limitations. For example, the “short-face” pigeon breeds have highly reduced premaxilla/beak size (see Supplementary Fig. 1), and are often incapable of feeding their hatchlings, requiring human intervention or surrogate parents to reach maturity. Similarly, the generation of short and curved beaks in domesticated breeds like the African owl creates functional limitations to jaw closure, which would help explain why birds with the greatest cranial or beak curvature more frequently have longer beaks. At the other extreme, avians with long beaks and unflexed crania are unsampled. This result may reflect the integrated

effects of a longer braincase and narrower frontal bones, suggesting either a requirement of additional neck musculature as a balancing mechanism, or a limitation on how narrow the frontal may become before affecting structural integrity. Given the relatively small changes of braincase shape relative to the face, this combination may be impacted by functional variation available in the braincase to match facial length.

The phylogenetic reconstructions within the shapespace represent testable hypotheses about both ancestral states and the developmental transformations underlying evolutionary trajectories between ancestral and descendant taxa. In the former case, the predictions of phylogenetic hypotheses are directly testable with the inclusion of plausible ancestral taxa from the fossil record into the morphospace. In the latter, the trajectories are plausibly linked to previously documented developmental determinants of beak shape in avians, providing potential experimental routes for testing mechanistic explanations for interspecific variation. For example, regulation of *Bmp4* expression during upper beak morphogenesis of phenotypically diverse species of the genus *Geospiza* impacts depth and width^{15,16}, while *Calmodulin* expression impacts length¹⁷. Variation in beak curvature may be responsive to differential regulation of local growth zones in the frontonasal mass by *Bmp4*^{18, 19}, or alternatively, is a product of how the inferior growth of the frontonasal mass interacts with the anterior extension of the maxillaries during primary palatal fusion²⁰. These determinants are also thought to exhibit modularity²¹, in that they have independent effects on beak shape, consistent with our results. Future studies could directly test these hypotheses by experimentally modulating the underlying developmental determinants associated with each axis in model species and comparing the phenotypic outcomes to the predictions of the avian shapespace.

The results support the hypothesis that a conserved developmental system is sufficient to explain the majority of avian craniofacial diversification. A recent analysis reached a similar conclusion in raptors, arguing that most observed variation in this group was due to either allometric scaling or non-allometric integration between the braincase and face, suggesting that developmental constraints have played an important role in the evolution of the raptor skull²². They further speculated that increasing modularity of the passerine skull might have enabled a greater relative diversification in songbirds. Although changes in clade-specific modularity may help explain relative differences in diversification, our results suggest that they are not necessary to explain diversification at the scale of all avians. Although the avian cranium is highly integrated, the magnitudes of correlated changes we identified in the braincase are small relative to those in the face (~1:3). Thus, while integration of the face and braincase influences craniofacial diversification as a whole, it does not appear to be a strict limit on the ability of the face to vary or evolve. Increased phylogenetic coverage of population-level variation of individual clades that vary widely in diversity would help to answer this question.

There are notable parallels between the patterns of variation and covariation described here and those described in the mammalian literature that suggest they are widely shared among amniotes. For example, analyses of craniofacial shape in domesticated dog breeds, wolves and carnivores found that the canine skull exhibits not only a similar pattern of integration and modularity between the face and brain, but also varies primarily in facial length, the

positioning of the face relative to braincase (i.e., cranial flexion), and the width of the skull²³. A similar distribution of shape variation has been observed in human craniofacial datasets^{24,25}. More broadly, Porto and colleagues performed a comparative analysis of genetic and phenotypic covariation in the skull of 15 mammalian orders, and found that "... both remained remarkably stable for a long evolutionary period, despite extensive morphological change and environmental shifts"²⁶. This stability in the pattern of variation and covariation between avians and mammals suggests that amniote craniofacial diversity varies and evolves within a shared space utilizing similar mechanisms and under similar constraints.

Why do amniote crania share a common pattern of variation and covariation? Covariation of traits within species occurs because of the correlated effects of variation in developmental processes⁸, and may result from directional selection operating on coordinated functional variation among traits¹². One possibility is that the embryonic bauplan of the head limits how structural components can be organized and vary relative to each other while maintaining functional relationships. In particular, the amniote brain is derived from the neural tube, while the face has its origin in prominences arranged around the developing brain (i.e., the frontonasal from nasal placodes and the maxillary from the first branchial arch, respectively), which grow together and fuse to form a continuous upper jaw²⁷. These relationships suggest the brain acts as a "platform" on which the face grows, with both structures influencing the other's development through molecular signals, structural interactions, and later somatic growth²⁸. Consequently, the width of the face is both dependent on brain size and is limited in where it is located (e.g., higher or lower), impacting overall curvature or flexion of the cranium. The increased integration of brain and face variation among the domestic pigeon breeds supports this argument. Similar integration of these features across amniotes therefore suggests a fundamental limitation on the generation of functional variation imposed by the structural design of the face:braincase complex, presumably primitive in the earliest vertebrates. Similar analyses of species with extreme craniofacial shapes that violate these rules may help to determine when and how these patterns are generated.

Darwin highlighted in his work the ability of humans to select in a short span of time pigeon breeds that mimicked or exceeded variation observed in wild doves. When considering the role of selection in domestication, he argued that "...in the construction of a building, mere stones or bricks are of little avail without the builder's art, so, in the production of new [breeds], selection has been the presiding power"¹. What Darwin could not appreciate at the time was that while breeders have wide latitude to generate variation, these variants mirror patterns of avian diversity at large. In the case of the avian cranium, and perhaps across vertebrates, we speculate that it is the embryonic architecture of the brain and face that shapes the space in which phenotypic diversity is possible, ultimately limiting the axes of functional variation that can be generated.

Methods

Data

To compare feral and domestic pigeons to proxies of the wildtype ancestral populations, we first obtained raw 2D linear distance data for the wild Rock Dove (*Columba livia*, Sardinia locality) (n=35), feral pigeons (combined North American and European populations) (n=91), and domesticated pigeon breeds (n=53) (see Supplementary Tab. 1)¹³. We next collected a sample of both feral (n=15) and domestic (n=58) pigeon skulls (see Supplementary Tab. 6), which were defleshed using dermestid beetles then scanned at a resolution of 40µm using micro-computed tomography (µCT) (Scanco Viva40). µCT scans were thresholded and converted into 3D objects in *Amira 5.6.0* (Visage Imaging, Inc.). Ferals were collected at a single locality (Arlington, Texas) and domestics from breeders located in both California and Texas. Domestic pigeons included the following breeds (n=36): Aachen Langer, African Owl, American Fantail, American Show Racer, Archangel, Berlin Long-Faced Tumbler, Birmingham “Wholly” Roller, Blondinette, Brunner Pouter, Budapest Shortface, Chinese Owl, Damascene, Dewlap, Domestic Show Flight, Egyptian Baghdad, English Carrier, English Short Face, German Beauty Homer, Hamburg Sticken, Helmet, Indian Fantail, Italian Owl, Lahore, Long-Face Clear Leg, Magpie, Maltese, Modena, Mooker, New York Flight, Polish Ice Tumbler, Polish srebniak, Roller, Scandaroon, Swallow, Vienna Medium Face, and West of England Tumbler.

To compare pigeon shape to the larger avian radiation, we next sampled avian crania (n=20) representing 16 orders and encompassing a range of beak shapes, sizes, and functions (Supplementary Fig. 8 and Supplementary Tab. 6): black-naped fruitdove (*Ptilinopus melanospilus*, Order: Columbiformes), kiwi (*Apteryx australis*, Order: Tinamiformes), ostrich (*Struthio camelus*, Order: Struthioniformes), chicken (*Gallus gallus*, Order: Galliformes), white pekin duck (*Anas platyrhynchos*, Order: Anseriformes), black vulture (*Coragyps atratus*, Order: Acciptriformes), bald eagle (*Haliaeetus leucocephalus*, Order: Acciptriformes), little penguin (*Eudyptula minor*, Order: Spheniciformes), emperor penguin (*Aptenodytes forsteri*, Order: Spheniciformes), Brandt's cormorant (*Phalacrocorax penicillatus*, Order: Pelecaniformes), frigatebird (*Fregata magnificens*, Order: Pelecaniformes), common loon (*Gavia immer*, Order: Gaviformes), giant hummingbird (*Patagona gigas*, Order: Caprimulgiformes), white-tipped sicklebill (*Eutoxeres aquila*, Order: Apodiformes), golden-winged parakeet (*Brotogeris chrysopterus*, Order: Psittaciformes), grebe (*Podilymbus podiceps*, Podicipediformes), albatross (*Diomedea exulans*, Order: Procellariiformes), auk (*Alca torda*, Order: Charadriiformes), red-tailed tropicbird (*Phaethon rubricauda*, Order: Phaethoniformes), and manakin (*Lepidothrix coronata*, Order: Passeriformes). Avian computed tomography (CT) data was obtained courtesy of the University of Texas High Resolution X-ray CT Facility (UTCT) (www.DigiMorph.org) (NSF Grant # IIS-0208675).

Linear Analysis

We first performed a reduced major axis (RMA) linear regression of cranial measurements on size (estimated as the geometric mean from both cranial and postcranial measurements). We tested for significant differences in elevation in the *smatR* module²⁹ implemented in the

software R^{30} . We next compared trait correlation structure via the matrix correlation (r_m), adjusted for repeatability (i.e., $r_{adjusted} = [r_{observed} / (t_a * t_b)^{0.5}]$, where t is the matrix repeatability of matrices a and b) resampling each population with replacement (10,000 replicates) to estimate autocorrelation), and tested for significance using Mantel's test³¹. To estimate and compare the magnitude of integration we calculated the variance of the eigenvalues (VE) for each correlation matrix^{32,33}. To control for the effect of sampled variance on correlation and eigenvalue estimates, we followed Young and colleagues³⁴ and resampled each population with replacement and recalculated VE and the average coefficient of variation (CV) of all cranial measurements for each replicate (10,000). We next calculated the log-linear relationship of CV to VE in those samples where $r_m > 0.95$ with the original matrix, and compared populations at similar CV values.

Shape Analysis

We next used geometric morphometric (GM) methods to quantify and compare shape variation and covariation among feral and domestic pigeons and the avian radiation. For each cranium we identified a series of 32 midline and bilaterally symmetric three-dimensional landmarks evenly divided between the face and braincase (see Supplementary Fig. 9 and Supplementary Tab. 7). Individual specimen coordinates (x, y, z) were located in the software *Landmark Editor* (v.3.5) using a semi-automated process that was repeated on two separate occasions. We compared between landmarking trials and noted low error, so we averaged coordinates between trials. We next performed a Procrustes superimposition on all the landmark data to remove the effects of scale, translation/location, and orientation. Data were averaged across the plane of bilateral symmetry to reduce dimensionality relative to sample size. We further averaged Procrustes data and centroid sizes within each breed and/or species to account for unequal sample sizes.

To test and control for significant size~shape allometry, we first calculated disparity and landmark variance for the entire craniofacial skeleton as well as within the braincase and face modules³⁵. We noted that facial shape variation was significantly increased whereas braincase shape was more conservative (Supplementary Fig. 10). We also collected published measures of body mass (BM) brain volume (BV) for all species in our analysis (see Supplementary Tab. 6). As previously demonstrated³⁶, brain~body allometry is significant in avians ($r^2 = 0.888$, $p < 0.0001$) (Supplementary Fig. 10), indicating brain volume is a good proxy for body mass. For the pigeon data, information on individual body mass was not collected, so we instead used braincase centroid size (BCS) as the measure of size. For comparisons among avians, we used \log BV as within cranium proxy to remain consistent with the pigeon analyses and to test for size~shape allometry in our cranial data. We performed a within-group multivariate regression of shape on BCS in pigeons (feral and domestic; see above). To compare between pigeon and avian brain~shape allometry, we centered average pigeon \log BV on the mean feral pigeon BCS.

To compare the distribution of shape variation and covariation in the non-allometric shape data, we performed a Principal Components Analysis (PCA) on residuals of brain~shape allometry. To compare overall covariation structure similarity we calculated the matrix correlation (r_m) and tested the hypothesis of no similarity using a permutation test (10,000

replicates). We further compared covariance structure by calculating the angle ($^{\circ}$) and vector correlation (r_v) between individual PCs and tested whether they were significantly better aligned than predicted by chance alone using a permutation test (1,000 iterations). To investigate integration and modularity of the face and braincase in the individual shape datasets, we performed a Partial Least Squares (PLS) analysis, estimated both the RV³⁷ and CR coefficients³⁸, and tested for significance using resampling procedures (200 replicates), utilizing the “integration.test” and “modularity.test” functions in the *R* package *geomorph*³⁹. We also tested for global integration following the method of Bookstein⁴⁰.

To estimate phylogenetic structure in our avian shape data, we generated 1,000 trees with molecular-derived branch lengths scaled to divergence times from www.birdtree.org⁴¹, calculated a majority-rule consensus tree in *Mesquite* v.3.10⁴² (see Supplementary Fig. 8), mapped the rooted tree in the PCA shape space weighted by branch lengths scaled to divergence time, and tested the hypothesis of no phylogenetic structure via a permutation test⁴³ and the *K* statistic^{44,45}. Occupation of shapespace over time was visualized by plotting PC1-2 against divergence time⁴⁶ as implemented in *geomorph*³⁹. Unless otherwise noted, all analyses were performed in *MorphoJ* v.1.06d⁴⁷ or the *geomorph* v.3.0.3 package³⁹ as implemented in *R*³⁰.

Data availability

Complete raw linear data is provided in the supplemental information (Supplementary Tab. S1). Avian computed tomography (CT) data is publicly available at www.digimorph.com. Phylogenetic data is publicly available at www.birdtree.org. Additional pigeon landmark and CT data that support the findings of this study are available from the corresponding author upon reasonable request.

Supplementary Material

Refer to Web version on PubMed Central for supplementary material.

Acknowledgments

We thank J. DeCarlo for kindly donating specimens of domestic pigeon breeds, A. Goode for preparing their skeletons, and R. Johnston for generously sharing his original pigeon data. Three anonymous reviewers provided helpful comments that greatly enhanced the manuscript. Non-pigeon avian CT data was provided courtesy of the University of Texas High Resolution X-ray CT Facility (UTCT) (NSF Grant # IIS-0208675). Research reported in this publication was supported by the National Institute of Dental and Craniofacial Research of the National Institutes of Health under Award Numbers F32DE018596 (NY), R01DE019638 (RM, BH), and R01DE021708 (RM, BH). The content is solely the responsibility of the authors and does not necessarily represent the official views of the National Institutes of Health.

References

1. Darwin, C. The Variation of Animals and Plants under Domestication. Vol. 1. John Murray; London: 1868.
2. Darwin, C. On the Origin of Species by Means of Natural Selection. John Murray; London: 1859.
3. Stringham SA, et al. Divergence, Convergence, and the Ancestry of Feral Populations in the Domestic Rock Pigeon. *Curr Biol*. 2012; 22:302–308. [PubMed: 22264611]
4. Shapiro MD. Genomic diversity and evolution of the head crest in the rock pigeon. *Science*. 2013; 339:1063–1067. [PubMed: 23371554]

5. Domyan ET, Shapiro MD. Pigeonetics takes flight: Evolution, development, and genetics of intraspecific variation. *Dev Biol.* xx:xxxx–xxxx. in press.
6. Wright S. Genic and organismic selection. *Evolution.* 1980; 34:825–843. [PubMed: 28581131]
7. Cheverud JM. Phenotypic, genetic, and environmental integration in the cranium. *Evolution.* 1982; 36:499–516. [PubMed: 28568050]
8. Hallgrímsson B, et al. Deciphering the Palimpsest: Studying the Relationship Between Morphological Integration and Phenotypic Covariation. *Evol Biol.* 2009; 36:355–376. [PubMed: 23293400]
9. Cheverud JM. 1996. Developmental integration and the evolution of pleiotropy. *Am Zool.* 1996; 36:44–50.
10. Wagner GP, Altenberg L. Complex adaptations and the evolution of evolvability. *Evolution.* 1996; 50:967–976. [PubMed: 28565291]
11. Maynard Smith J, et al. Developmental constraints and evolution. *Quart Rev Biol.* 1985; 60:265–287.
12. Wagner GP, Pavlicev M, Cheverud J. The road to modularity. *Nat Rev Genet.* 2007; 8:921–931. [PubMed: 18007649]
13. Johnston RF. Evolution in the Rock Dove: Skeletal Morphology. *Auk.* 1992; 109:530–542.
14. Baptista LF, Gomez Martinez JE, Horblit HM. Darwin's pigeons and the evolution of the columbiforms: recapitulation of ancient genes. *Acta Zool Mex.* 2009; 25:719–741.
15. Abzhanov A, et al. *Bmp4* and Morphological Variation of Beaks in Darwin's Finches. *Science.* 2004; 305:1462–1465. [PubMed: 15353802]
16. Wu P, et al. Molecular Shaping of the Beak. *Science.* 2004; 305:1465–1466. [PubMed: 15353803]
17. Abzhanov A, et al. The calmodulin pathway and evolution of elongated beak morphology in Darwin's finches. *Nature.* 2006; 442:563–567. [PubMed: 16885984]
18. Wu P, et al. Morphoregulation of Avian Beaks: Comparative Mapping of Growth Zone Activities and Morphological Evolution. *Dev Dyn.* 2006; 235:1400–1412. [PubMed: 16586442]
19. Fritz JA, et al. Shared developmental programme strongly constrains beak shape diversity in songbirds. *Nat Comm.* 2015; 5:3700.
20. Linde-Medina M, Newman SA. Limb, tooth, beak: Three modes of development and evolutionary innovation of form. *J Biosci.* 2014; 39:211–223. [PubMed: 24736155]
21. Mallarino R, et al. Two developmental modules establish 3D beak-shape variation in Darwin's finches. *Proc Natl Acad Sci USA.* 108:4057–4062.
22. Bright JA, et al. The shapes of bird beaks are highly controlled by nondietary factors. *Proc Natl Acad Sci USA.* 2016; 113:5352–5357. [PubMed: 27125856]
23. Drake AG, Klingenberg CP. Large-Scale Diversification of Skull Shape in Domestic Dogs: Disparity and Modularity. *Am Nat.* 2010; 175:289–301. [PubMed: 20095825]
24. Martínez-Abadías N, et al. Pervasive Genetic Integration Directs the Evolution of Human Skull Shape. *Evolution.* 2010; 66:1010–1023.
25. Young NM, et al. Facial surface morphology predicts variation in internal skeletal shape. *Am J Orthod Dent Orthop.* 2016; 149:501–508.
26. Porto A, et al. The Evolution of Modularity in the Mammalian Skull I: Morphological Integration Patterns and Magnitudes. *Evol Biol.* 2009; 36:118–135.
27. Young NM, et al. Embryonic bauplans and the developmental origins of facial diversity and constraint. *Development.* 2014; 141:1059–1063. [PubMed: 24550113]
28. Marcucio RS, Young NM, Hu D, Hallgrímsson B. Mechanisms that Underlie Co-variation of the Brain and Face. *Genesis.* 2011; 49:177–189. [PubMed: 21381182]
29. Warton DI, et al. *smatr 3* - an R package for estimation and inference about allometric lines. *Meth Ecol Evol.* 2012; 3:257–259.
30. R Core Team. R: A language and environment for statistical computing. R Foundation for Statistical Computing; 2016. Vienna, Austria. URL <https://www.R-project.org/>
31. Marroig G, Cheverud JM. A comparison of phenotypic variation and covariation patterns and the role of phylogeny, ecology, and ontogeny during cranial evolution of new world monkeys. *Evolution.* 2001; 55:2576–2600. [PubMed: 11831671]

32. Wagner GP. On the eigenvalue distribution of genetic and phenotypic dispersion matrices: Evidence for a non-random origin of quantitative genetic variation. *J Math Biol.* 1984; 21:77–95.
33. Pavlicev M, Cheverud JM, Wagner GP. Measuring Morphological Integration Using Eigenvalue Variance. *Evol Biol.* 2009; 36:157.
34. Young NM, Wagner GP, Hallgrímsson B. Development and the evolvability of human limbs. *Proc Natl Acad Sci USA.* 2010; 107:3400–3405. [PubMed: 20133636]
35. Zelditch, ML., Swiderski, DL., Sheets, HD. Geometric morphometrics for biologists: a primer. Academic Press; 2012.
36. Nealen PM, Ricklefs R. Early diversification of the avian brain:body relationship. *J Zool Lond.* 2001; 253:391–404.
37. Klingenberg CP. Morphometric integration and modularity in configurations of landmarks: tools for evaluating a priori hypotheses. *Evol Dev.* 2009; 11:405–421. [PubMed: 19601974]
38. Adams DC. Evaluating modularity in morphometric data: Challenges with the RV coefficient and a new test measure. *Meth Ecol Evol.* 2016; 7:565–572.
39. Adams DC, Otárola-Castillo E. geomorph: an R package for the collection and analysis of geometric morphometric shape data. *Meth Ecol Evol.* 2013; 4:393–399.
40. Bookstein FL. Integration, disintegration, and self-similarity: Characterizing the scales of shape variation in landmark data. *Evol Biol.* 2015; 42:395–426. [PubMed: 26586921]
41. Jetz W, et al. The global diversity of birds in space and time. *Nature.* 2012; 491:444–448. [PubMed: 23123857]
42. Maddison, WP., Maddison, DR. Mesquite: a modular system for evolutionary analysis. Version 3.10. 2016. <http://mesquiteproject.org>
43. Klingenberg CP, Gidaszewski NA. Testing and quantifying phylogenetic signals and homoplasy in morphometric data. *Syst Biol.* 2010; 59:245–261. [PubMed: 20525633]
44. Blomberg SP, Garland T, Ives AR. Testing for phylogenetic signal in comparative data: behavioral traits are more labile. *Evolution.* 2003; 57:717–745. [PubMed: 12778543]
45. Adams DC. A generalized Kappa statistic for estimating phylogenetic signal from shape and other high-dimensional multivariate data. *Syst Biol.* 2014; 63:685–697. [PubMed: 24789073]
46. Sakamoto M, Ruta M. Convergence and Divergence in the Evolution of Cat Skulls: Temporal and Spatial Patterns of Morphological Diversity. *PLoS ONE.* 2012; 7:e39752. [PubMed: 22792186]
47. Klingenberg CP. MorphoJ: an integrated software package for geometric morphometrics. *Mol Ecol Res.* 2011; 11:353–357.

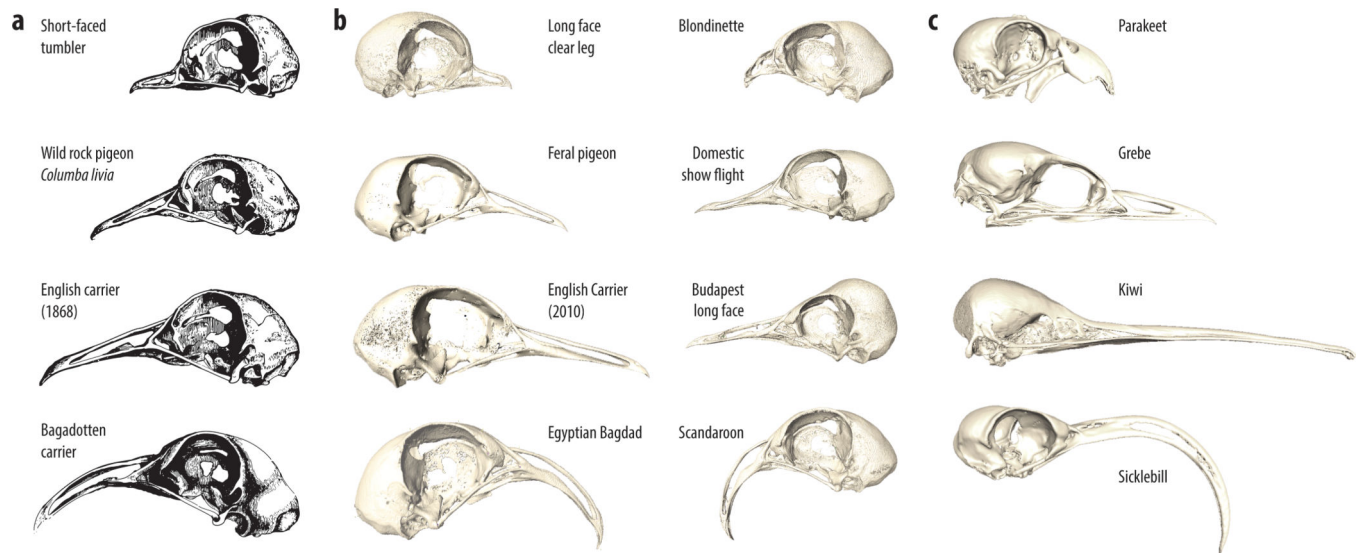


Figure 1. Variation in the pigeon craniofacial skeleton compared to avian diversity
a, Original examples of domesticated pigeon breed diversity from Darwin¹. **b**, Modern examples (left) illustrate notable breed variants examined in this study (see Supplementary Fig. 1 for a complete list). Examples of pigeon breeds with extreme craniofacial shapes (right) qualitatively converge on distantly related avians. **c**, Examples of avian crania with shape characteristics similar to domesticated pigeon breeds (individual crania shown scaled to similar braincase length).

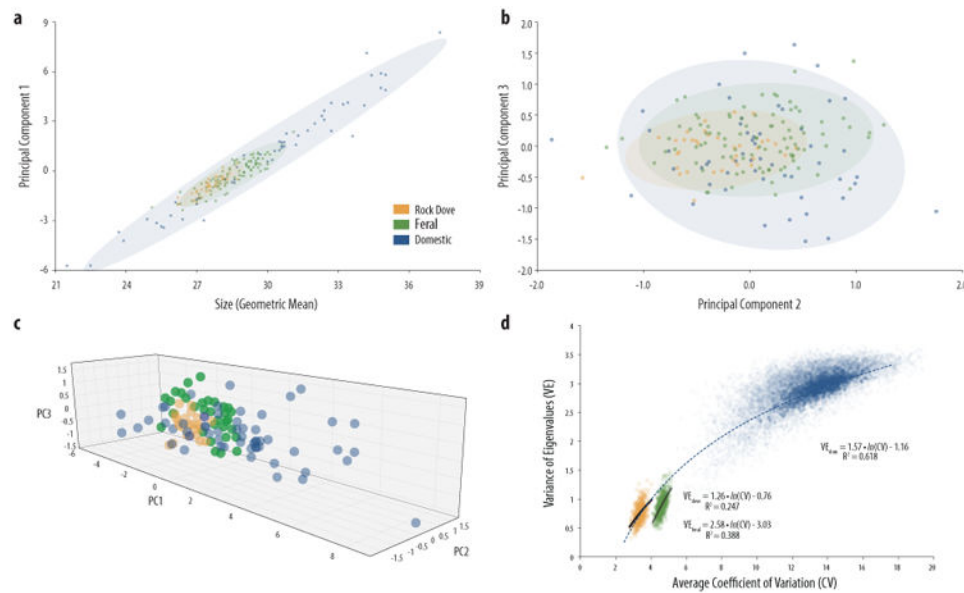


Figure 2. Results of the Principal Components Analysis (PCA) from linear distance data
a-c, Feral and domestic pigeon breeds reflect a nested pattern of covariation with the ancestral rock dove (*Columba livia*) but have increased variation along these commonly held axes. Rock Dove = orange; Feral = green; Domestic = blue. 90% equal frequency ellipses shown. **d**, Overall magnitude of integration is similar in rock doves and ferals. Domestic breed integration is comparable after controlling for variation. Curves illustrate *log*-linear regressions for resampled populations (10,000 replicates).

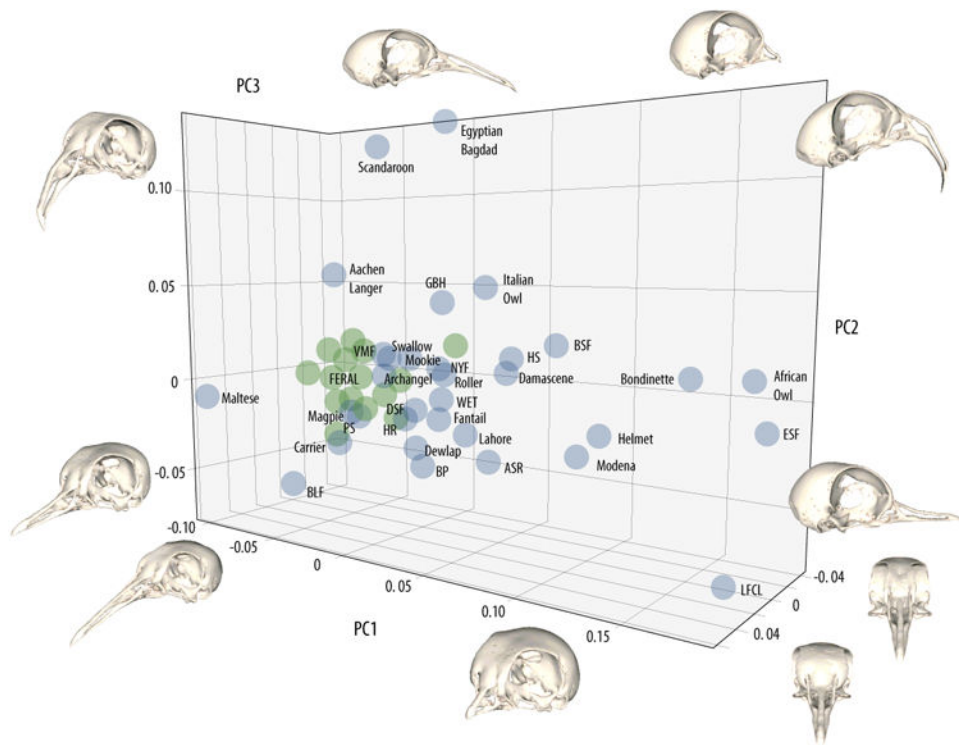


Figure 3. Pigeon craniofacial shape morphospace

Results of the Principal Components Analysis (PCA) showing the first three axes. The mean sample cranium is shown warped to maximum positive and negative values along each axis. PC1 (top, lateral view; bottom, oblique view) distinguishes between short (brachycephalic) and long (dolichocephalic) crania, largely due to extension of the beak skeleton (i.e., premaxilla) (64.2% total variation). PC2 (left, oblique view; right, lateral view) discriminates curved beaks located higher on the braincase with a flexed basicranium from crania in which the beak is straighter and located lower on the braincase with a flat basicranium (16.7% total variation). PC3 (bottom right, frontal view) discriminates between the width of the frontal bone and the space separating the orbits (5.4% total variation). Feral pigeons = green, domestic breeds = blue. Labels identify breeds.

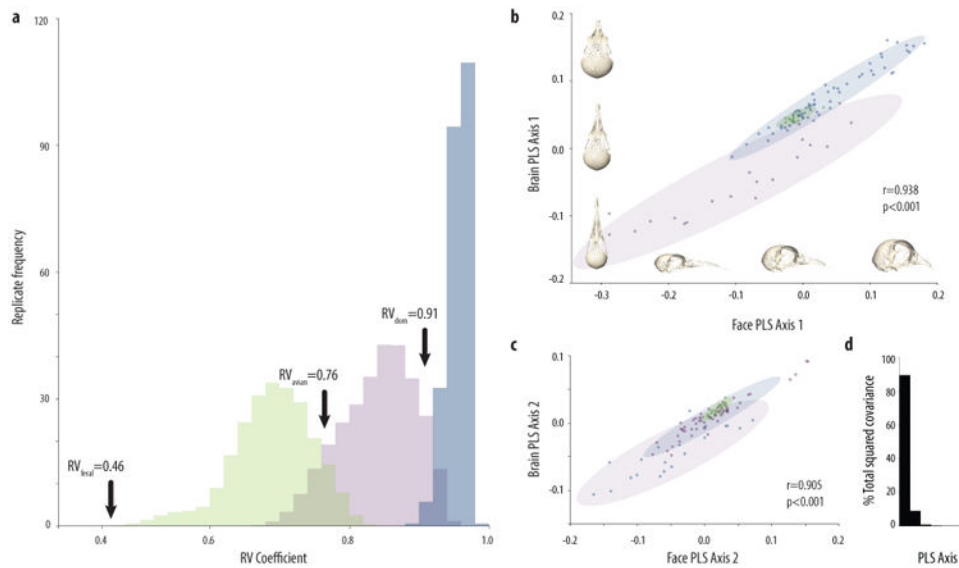


Figure 4. Results of the Partial Least Squares (PLS) analysis of face and braincase modules
a, RV estimates relative to resampled distributions for ferals (green), domestics (blue), and avians (purple) indicate face and braincase modularity. **b-c**, PLS1-2 axes are consistent with strong integration associated with craniofacial length and width. **d**, The majority of covariation between the avian and pigeon face and brain is explained by the first PLS axis.

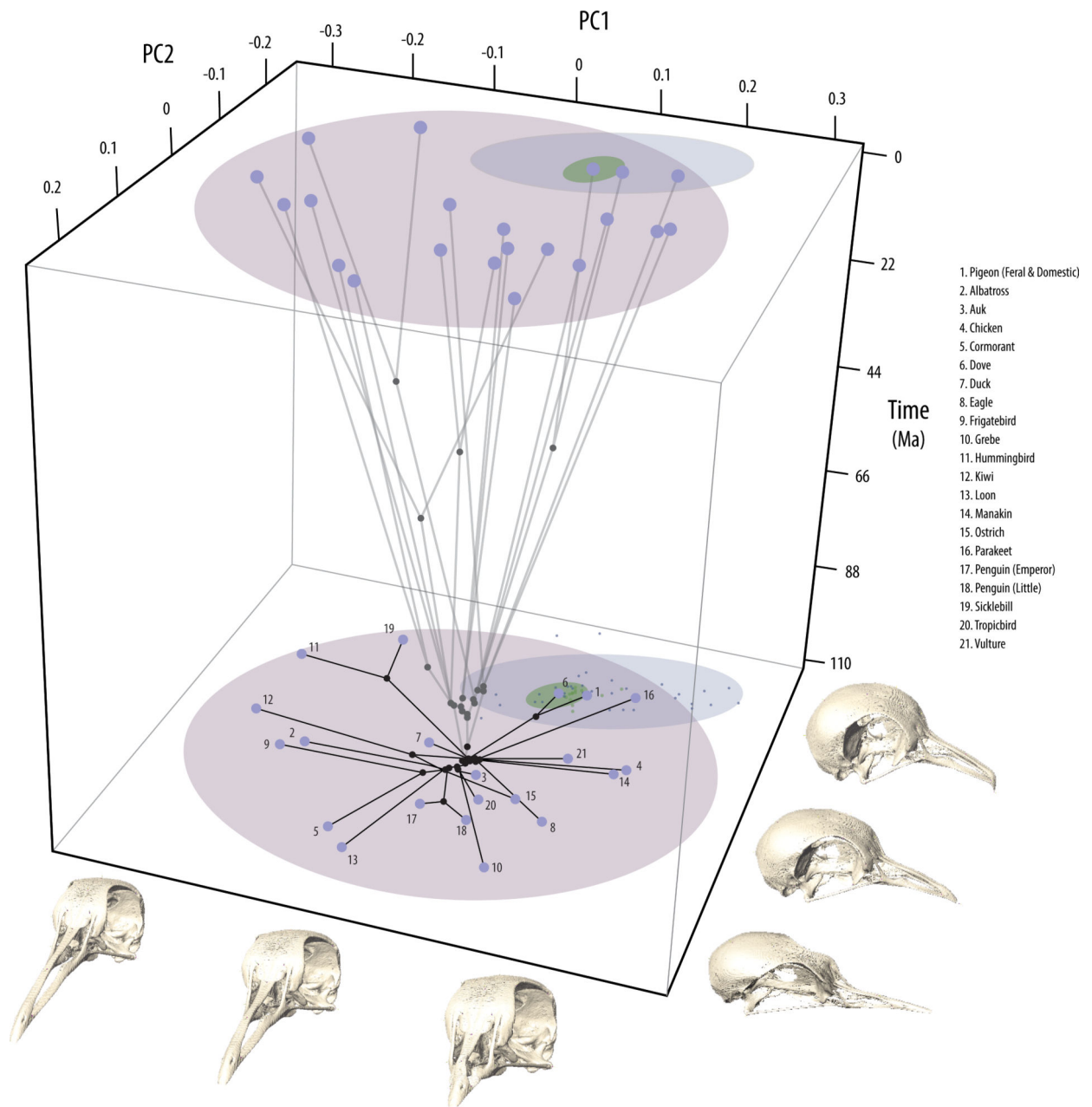


Figure 5. Comparison of craniofacial diversification in domesticated pigeon breeds with the avian radiation

The Principal Components Analysis (PCA) results illustrated as a “chronophylomorphospace”⁴⁶ with reconstructed phylogenetic branching pattern and ancestral states (grey) shown relative to divergence time (vertical axis). Domesticated pigeons (blue) overlap the fruit dove and the short-beaked parakeet. Domesticates have diversified relative to ferals (green) over 10,000 years of artificial selection in a pattern mirroring avians (purple) as a whole, but not as extensively. Warped specimens on each axis illustrate associated shape transformations: PC1 describes beak length, while PC2 is

associated with cranial flexion/curvature and brain width. The morphospace exhibits significant phylogenetic structure ($K=0.895$, $p=0.042$) (Supplementary Fig. 6).

Author Manuscript

Author Manuscript

Author Manuscript

Author Manuscript